Low-rank representation for reflectivity model and its applications in least-squares migration

Jidong Yang, Jianping Huang, China University of Petroleum (East China); Hejun Zhu, George McMechan, The University of Texas at Dallas

SUMMARY

We investigate both global and local low-rank representations for seismic reflectivity models. Within the global singular value decomposition (SVD) framework, singular vectors delineate elementary modes representing horizontal and vertical stratigraphic segments, while corresponding singular values serve as weights for these fundamental modes, collectively forming a broadband reflectivity model. Local SVD, on the other hand, captures nonlocal similarities and achieves reflectivity representation with fewer ranks than global SVD method. Taking advantage of this favorable sparsity, we introduce a local low-rank regularization into LSM to estimate subsurface reflectivity models. Numerical experiments for synthetic and field data demonstrate that the low-rank constraint outperforms conventional shaping and total-variation regularizations, and can produce high-quality reflectivity images for complicated structures.

INTRODUCTION

Tectonic movements and sedimentary processes give rise to diverse subsurface strata, featuring fundamental elements like horizontal and dipping layers, angular unconformities, pinch-outs, folds and faults. These distinctive characteristics lead to nonlocal similarities in seismic reflectivity models, which can be sparsely represented through suitable basis functions. In this study, we explore global and local low-rank representations for reflectivity models. In global singular value decomposition (SVD) approach, we observe that eigenvectors delineate horizontal and vertical stratigraphic segments sorted from low to high wavenumbers, with corresponding eigenvalues serving as weights for assembling these eigenvectors into a broadband reflectivity model. In contrast, the local SVD for grouped patches can effectively capture nonlocal geological patterns. This capability enables accurate description of subsurface reflectivity using fewer ranks compared to the global SVD method.

Seismic imaging serves as a crucial tool for reconstructing subsurface reflectivity by migrating seismic data acquired at the surface into the depths below. Over time, seismic imaging methods have evolved from ray-based migration (Gray and May, 1994), through one-way wave equation migration (Gazdag, 1978; Stoffa et al., 1990), to advanced reverse-time migration (RTM) (McMechan, 1983). These methods utilize the adjoint operator of forward modeling rather than the inverse operator, posing challenges in achieving accurate images, particularly in scenarios with finite acquisition aperture, limited frequency bands and uneven illumination. By solving a linear inverse problem, least-squares migration (LSM) can reduce the Hessian effect and improve the image quality (Nemeth et al., 1999; Dai et al., 2011). To mitigate data overfitting artifacts, various regularization strategies have been developed, including shaping regularizations (Xue et al., 2016; Yang et al., 2021), curvelet-domain sparsity promotion (Herrmann and Li, 2012), and total-variation (TV) regularization (Lin and Huang, 2015). Taking advantage of local low-rank sparse representation, we introduce a low-rank regularization into LSM to estimate subsurface reflectivity. A two-step framework, including least-squares data fitting and weighted nuclear-norm minimization, is utilized to solve the low-rank constrained inversion problem. Numerical experiments for synthetic and field data demonstrate that the low-rank constraint outperforms traditional smoothing and TV regularizations to generate high-quality reflectivity images for complicated structures.

THEORY

Global low-rank representation

Seismic reflectivity model can be converted into a matrix by setting the depth as the first dimension and the inline or cross line as the second dimension. Then, applying the SVD to the matrix leads to

$$\mathbf{m} = \mathbf{U}\mathbf{\Sigma}\mathbf{V}^T, \tag{1}$$

where $\mathbf{m}$ represents a reflectivity matrix, $\mathbf{U}$ and $\mathbf{V}$ are the left and right singular matrices, and $\mathbf{\Sigma}$ is the diagonal singular value matrix. The columns of $\mathbf{U}$ and $\mathbf{V}$ correspond to the base vectors of the coordinate system, which determine the elementary modes of the reflectivity model with different wavenumbers. The singular values describe the contribution of these modes to construct a broadband reflectivity profile. If the reflectivity matrix has few linearly independent columns, it can be efficiently represented using a low-rank approximation by truncating small singular values or minimizing the matrix nuclear norm. In a truncated SVD, the reflectivity model can be approximated as

$$\mathbf{m}' \approx \mathbf{U}_k\mathbf{\Sigma}_k\mathbf{V}_k^T, \tag{2}$$

where $\mathbf{\Sigma}_k$ denotes a modified singular value matrix by setting all but the first k largest singular values to zero, where $\mathbf{U}_k$ and $\mathbf{V}_k$ mean that only their first k columns are used in the calculation. On the other hand, the low-rank representation can be implemented by minimizing

the matrix nuclear norm:

$$\chi(\mathbf{m}) = \frac{1}{2}||\mathbf{m}_{cal} - \mathbf{m}||^2 + \lambda||\mathbf{m}||_*, \quad (3)$$

where $\mathbf{m}_{cal}$ is the calculated reflectivity model using seismic migration. $||\mathbf{m}||_* = \sum_i \sigma_i$ denotes the nuclear norm, σ_i is the singular value, and λ is a scalar that controls the trade-off between data fitting and nuclear norm regularization.

Local low-rank representation

Local low-rank representation applies SVD to a series of grouped reflectivity patches, which can effectively capture the nonlocal similarity and local sparsity (Zhang et al., 2014). The detailed steps of local low-rank representation are as follows.

1. The reflectivity model $\mathbf{m}$ is divided into a series of overlapped local patches, i.e., $\mathbf{m}_i$ $(i = 1, 2, ..., N)$, where N is the total number of patches.
2. For each patch $\mathbf{m}_i$, the most similar M neighboring patches are selected from an $L \times L$ window to form a patch group with the elements of $\mathbf{g}_{i,j}$ $(j = 1, 2, ..., M)$.
3. By reshaping the patch $\mathbf{g}_{i,j}$ into vectors, we can construct a matrix $\mathbf{m}'_i$ using these vectors as columns, i.e., $\mathbf{m}'_i = [\mathbf{g}_{i,1}, \mathbf{g}_{i,2}, \mathbf{g}_{i,3}, ..., \mathbf{g}_{i,M}]$.
4. We apply SVD to these local reflectivity matrices as
$$\mathbf{m}'_i = \mathbf{U}_i\mathbf{\Sigma}_i\mathbf{V}_i^T, \quad (4)$$
where the subscript i denotes the local SVD result of the ith group of patches.

Similar to the global method, the local low-rank approximation for the reflectivity model can be implemented by using truncated SVD or nuclear norm minimization. Since the grouped patches consist of many similar structures, the local SVD in equation 4 has a better low-rank property than the global SVD shown in equation 2.

Low-rank regularized LSM

We apply the local low-rank constraint to LSM to improve its adaptability for complex structures, which is implemented by minimizing the weighted nuclear norm of reflectivity patch matrices. The corresponding misfit function can be expressed as

$$\chi = \frac{1}{2}\|\mathbf{L}\mathbf{m} - \mathbf{d}_{obs}\|^2 + \|\mathbf{m}\|_{\mathbf{w},*}, \quad (5)$$

where $\mathbf{L}$ denotes the Born modeling in acoustic or viscoacoustic media, $\|\mathbf{m}\|_{\mathbf{w},*} = \sum_i \|\mathbf{m}'_i\|_{\mathbf{w},*} = \sum_{i,j} w_{i,j}\sigma_{i,j}$ is the weighted nuclear norm, $\mathbf{m}'_i$ denotes the i^{th} matrix constructed from local grouped patches that are extracted from the expected reflectivity model $\mathbf{m}$ as described in the low-rank representation section, $\sigma_{i,j}$ is the j^{th} singular value of $\mathbf{m}'_i$, and $\mathbf{w} = [w_{i,1}, w_{i,2}, ..., w_{i,j}]$ is a non-negative weight assigned for $\sigma_{i,j}$.

The optimization problem with a sparse constraint in equation 5 can be solved using a two-step algorithm (Yang et al., 2019). The first step is to solve a traditional least-squares problem as

$$\mathbf{m}_1 = \arg\min_{\mathbf{m}} \frac{1}{2}\|\mathbf{L}\mathbf{m} - \mathbf{d}_{obs}\|^2, \quad (6)$$

which can be computed by using the preconditioned conjugate gradient method. With the solution of $\mathbf{m}_1$, the second step is to solve the following problem

$$\mathbf{m}_2 = \arg\min_{\mathbf{m}} \frac{1}{2}\|\mathbf{m} - \mathbf{m}_1\|^2 + \|\mathbf{m}\|_{\mathbf{w},*}. \quad (7)$$

For each grouped patch matrix, the solution of equation 7 can be calculated by applying a soft thresholding to the singular values as

$$\hat{\sigma}_{i,j} = \max\left(\sigma_{i,j} - w_{i,j}, 0\right), \quad (8)$$

and then the matrix is recovered as

$$\hat{\mathbf{m}'}_i = \mathbf{U}_i\hat{\mathbf{\Sigma}}_i\mathbf{V}_i, \quad \hat{\mathbf{\Sigma}}_i = diag\left[\hat{\sigma}_{i,1}, \hat{\sigma}_{i,2}, ..., \hat{\sigma}_{i,j}\right], \quad (9)$$

where $\sigma_{i,j}$ is the j^{th} singular value of the i^{th} patch matrix $\mathbf{m}'_i$ extracted from $\mathbf{m}_1$, and $\mathbf{U}_i$ and $\mathbf{V}_i$ are the left and right singular matrices of $\mathbf{m}'_i$, respectively. Following Zha et al. (2017), we choose the weight function as

$$\mathbf{w}_i = \frac{2\sqrt{2}\kappa^2}{\gamma_i + \epsilon}, \quad (10)$$

where κ is an input parameter to control the strength of the low-rank constraint, γ_i is the estimated standard variance of the singular values in the ith group, and ϵ is a small constant to avoid division by zero. The complete reflectivity model is reconstructed by aggregating all the group matrices $\hat{\mathbf{m}'}_i$.

NUMERICAL EXAMPLES

We first use the benchmark Marmousi model to test the feasibility of the proposed method, which is resampled with a 10-m increment onto a grid of 1943×401. 144 sources are evenly deployed on the surface with a 100-m interval, and each source is recorded by 501 receivers in a 5-km split-spread aperture. The time sample increment of records is 4 ms and the duration is 4 s. A 12-Hz Ricker wavelet is used as the source time function. Viscoacoustic modeling is employed to compute common-source gathers, after which random noise is added to simulate a low signal-to-noise ratio (SNR) dataset. Migration results and detailed comparisons are shown in Figures 1-2.

RTM produces good images for shallow reflectors, but deep layers exhibit much weak amplitudes due to unbalanced illumination (Figure 1a). Through correction of the Hessian effect, LSRTM enhances deep amplitudes and improves image resolution, but the inversion process aggravates the contamination of random noise (Figures 1b and 2a, b). This is because LSRTM not only fits

effective reflections but also tries to fit noises. Although the shaping regularization partially improve the SNR of shallow layers, the deep image is still seriously degraded (Figure 1c). Even worse, it may convert random noise to coherent noise by structural-dependent smoothing (Figures 2c, d). TV-regularized LSM removes most random noise and produces a clearer image than traditional LSM (Figure 1d). One drawback is that it might generate speckle artifacts and break event continuity (Figures 2e and f). In contrast, low-rank regularized LSM completely removes the adverse influence of random noise and produces a high-quality image similar to the result from clean data (Figures 1e and 2g, h).

In the second example, we apply the proposed method to a field data of a land survey. 70 common-shot gathers are recorded along a 2D survey line with an average source increment of 175 m. Receiver numbers range from 567 to 706 for different sources, with an average spacing of 25 m and a maximum offset of 7.11 km. The time sampling is 2 ms and the record duration is 6 s. Preprocessings, including direct wave muting, surface wave attenuation, bad trace removal, amplitude correction from 3D to 2D and bandpass filtering, are applied to common-shot gathers before migration. A representative gathers are shown in Figure 3. Migration results are presented in Figure 4. On the RTM image, horizontal reflectors are imaged clearly, but deeper reflectors in the sedimentary basin and its dipping flank are not well resolved (Figure 4a). With ten iterations, LSRTM significantly enhances the amplitudes of the deep reflectors and improves the image resolution, but it increases the image noise level (Figure 4b). TV-regularized LSM has a good denoising performance, but generates some nonphysical speckled artifacts below the basin basement (Figure 4c). Low-rank regularization removes most random noise and does not generate additional artifacts (Figure 4d). Both shallow fine layers and deep strong reflectors are imaged clearly, and the basin flank and basement are well defined.

CONCLUSION

In this study, we introduce a local low-rank constraint into the LSM framework for reflectivity inversion. A two-step method is developed to solve the low-rank regularized inverse problem: the first step is for least-squares data fitting using the preconditioned conjugate gradient method, and the second step is for minimizing the weighted nuclear norm using adaptive soft thresholding. Numerical experiments on synthetic and field data demonstrate that low-rank regularized LSM outperforms shaping and TV regularizations in improving image SNR and spatial resolution.

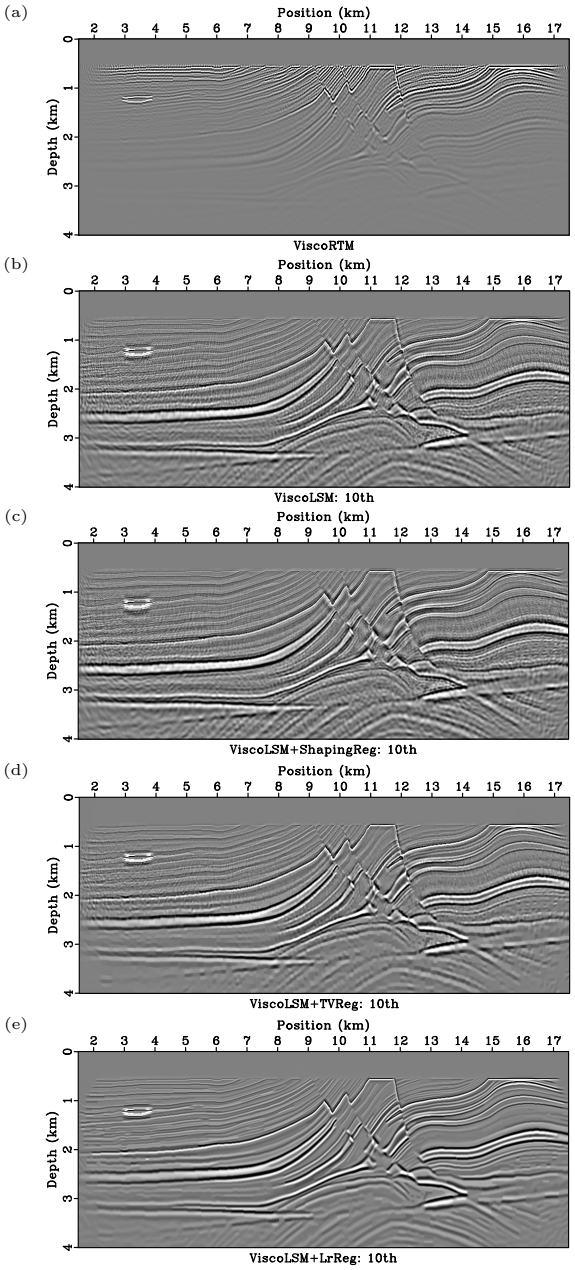

Figure 1: Migration results of the Marmousi model with noisy viscoacoustic data (SNR = 1). (a) Preconditioned viscoacoustic RTM with source illumination, (b) viscoacoustic LSM without regularization, (c) viscoacoustic LSM with shaping regularization, (d) viscoacoustic LSM with TV regularization, (e) viscoacoustic LSM with low-rank regularization, and (f) viscoacoustic LSM with low-rank and shaping regularizations. The signal-to-noise-ratio of (b)-(f) are 1.72 dB, 2.14 dB, 4.11 dB, 4.42 dB, 3.82 dB, respectively.

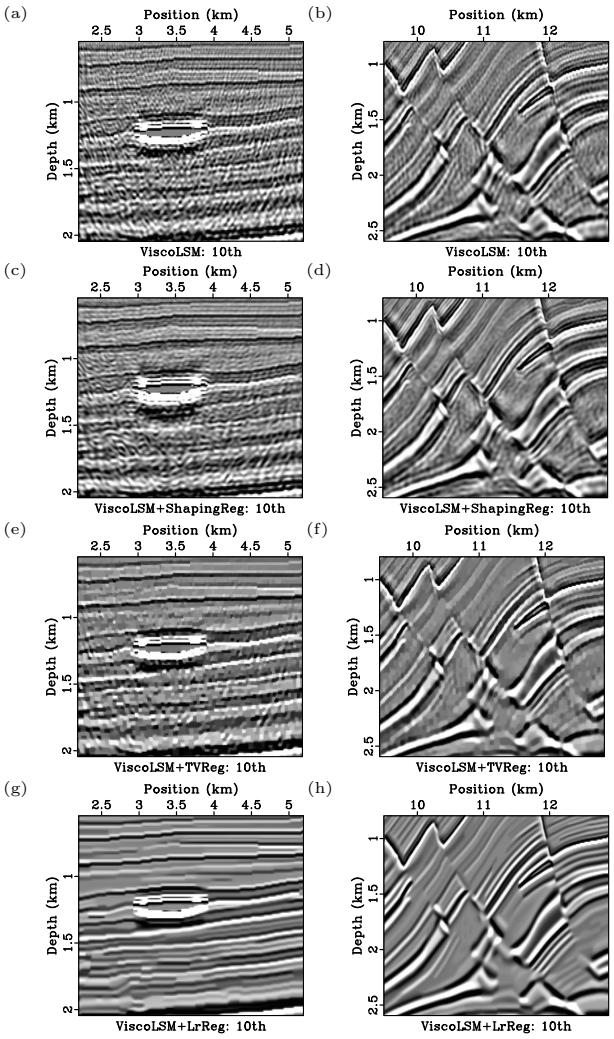

Figure 2: Enlarged local migration results of the Marmousi model with noisy data. (a, c, e, g) are for x=[2.2 km, 5.5 km] and z=[0.55 km, 2.55 km], (b, d, f, h) are for x=[9.5 km, 12.8 km] and z=[0.8 km, 2.6 km]. Four rows are LSMs without regularization and with shaping, TV, and low-rank regularizations, respectively.

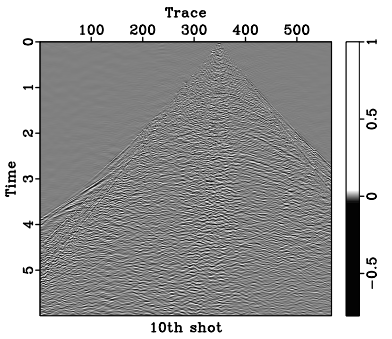

Figure 3: A representative common-source gathers from the land survey.

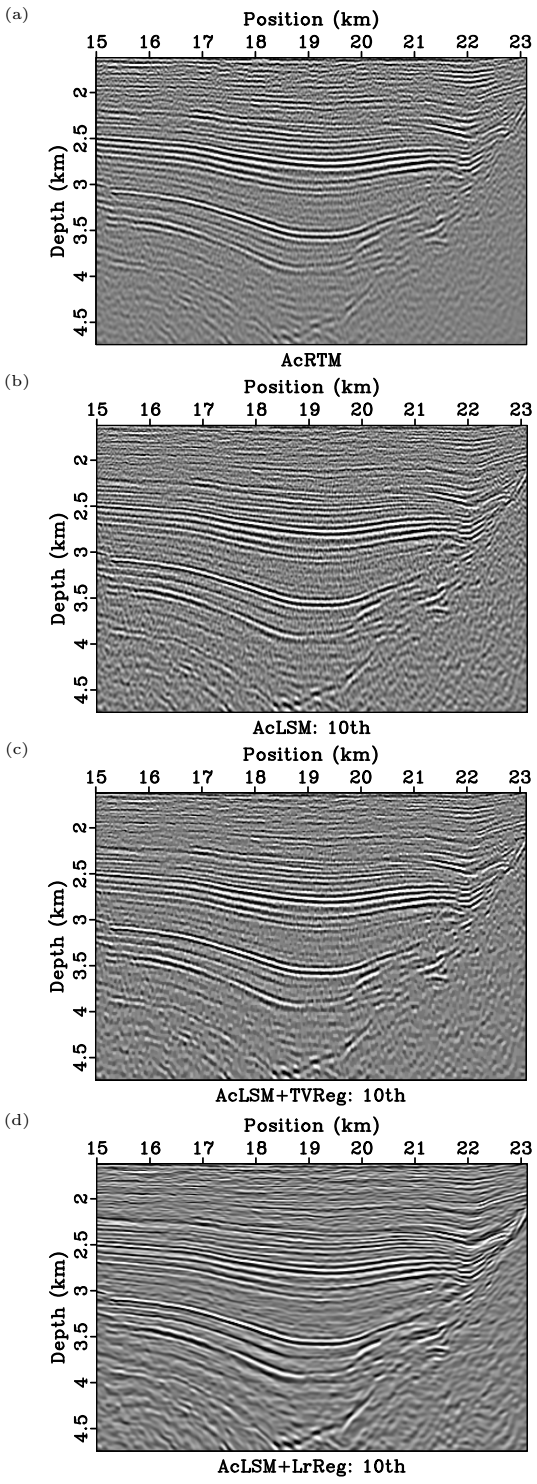

Figure 4: Migration results of field data using an acoustic propagator. (a) RTM, (b) LSM without regularization, (c) LSM with shaping regularization, (d) LSM with TV regularization, (e) LSM with low-rank regularization, and (f) LSM with low-rank and shaping regularizations.